Estimation of Tropical Cyclone Intensity by Remote Sensing

This information has been summarised from the Introduction to Tropical Meteorology (2nd Edition) which can be accessed, free of charge, on the [MetEd/ COMET website](#) (requires free registration).

Remote-sensing is the primary method of observing tropical cyclones, which spend most of their lifetime over the ocean, outside of the network of in-situ instruments. In addition to estimates of intensity, remotely-sensed observations help scientists to understand the large-scale environment and Tropical Cyclone (TC) internal instabilities, factors which influence tropical cyclone intensity.

Instruments include satellite radiometers (infrared (IR), visible, and microwave), precipitation and cloud radars (ground, airborne, and satellite), satellite scatterometers, and synthetic aperture radars (SAR). Figure 1 illustrates recent advances in satellite radar and microwave observations of tropical cyclone structure.

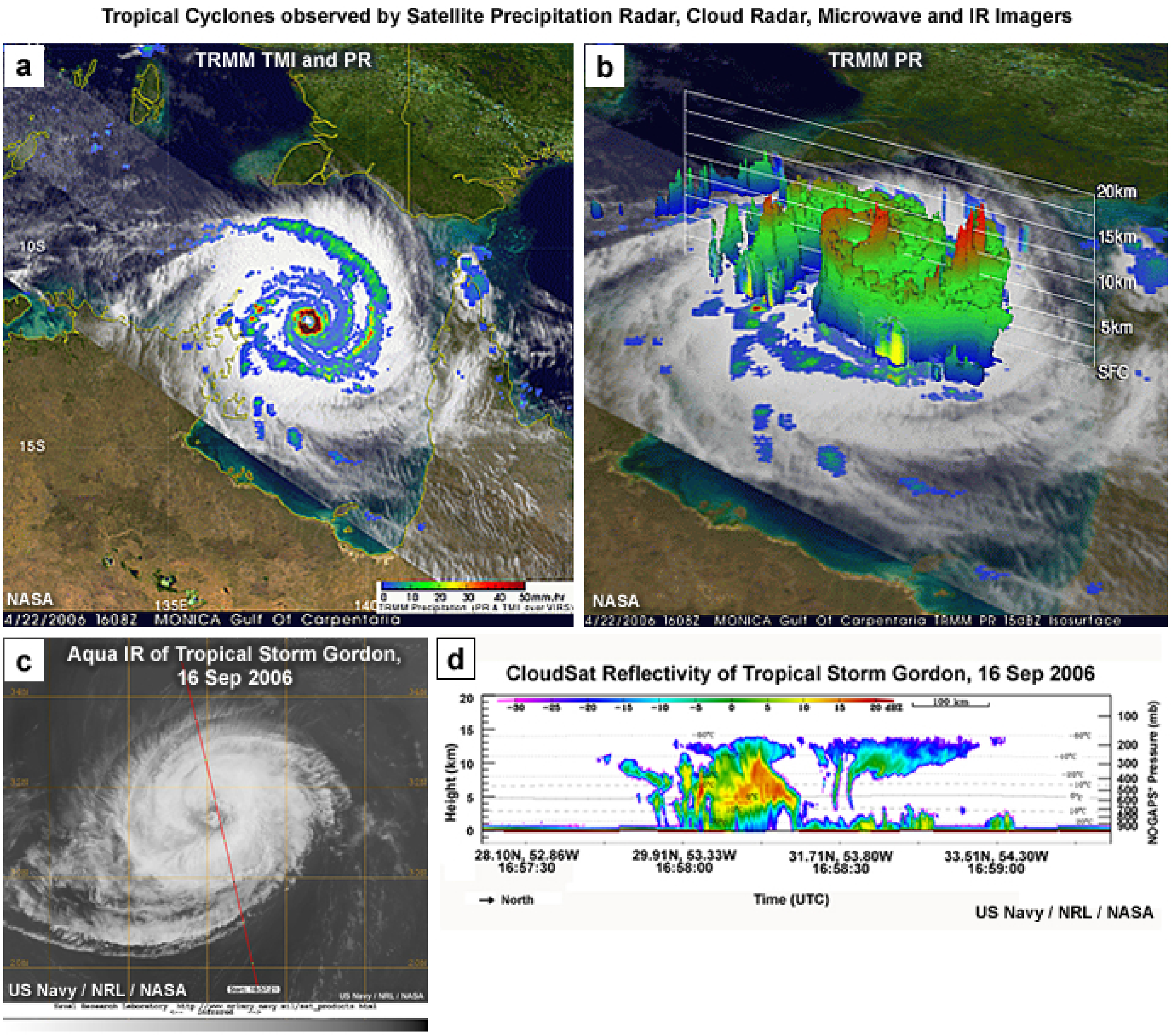

Figure 1 Tropical cyclone satellite observations: (a) the Tropical Rainfall Measurement Mission (TRMM) Precipitation Radar (PR), TRMM Microwave Imager (TMI), and Visible Infrared Scanner (VIRS); (b) 3D radar reflectivity from the TRMM PR; (c) Aqua-EOS IR; and (d

Satellite-IR Estimates

The standard method of estimating TC intensity is by analysing geostationary longwave (IR) images, except for the North Atlantic and Northeast Pacific, where aircraft reconnaissance flights are routine. With frequently available geostationary IR images (15-30 minutes routinely and 5 minutes in rapid-scan mode), the intensity can be updated for continuous operational forecasting.

In 1975, Vern Dvorak introduced a classification scheme for estimating the intensity of TCs from satellite imagery. The 'Dvorak Technique', which was developed using empirical data, relates a numerical index (called the current intensity or CI) to an estimate of the maximum sustained winds (MSW) at the surface (Table 1).

The Dvorak Enhanced IR technique uses a special enhancement, known as the IR-BD curve, to identify intense convection and changes in the cloud top pattern around the eye. It identifies four basic TC pattern types, the:

- Eye pattern
- Curved band pattern
- Shear pattern
- Central dense overcast (CDO) pattern

The eye pattern identifies the temperature contrast between the warmest part of the eye and the coldest surrounding convection within 55 km (e.g., Fig. 2). The greater the temperature contrast, the stronger the system.

The curved band pattern is based on the idea that the more wrapped around the rainbands, the greater the system vorticity. The curved band pattern is often easier to follow in visible images than in IR images.

The CDO is the area covered by the cirrus clouds that extend from thunderstorms in the eyewall and rainbands of a TC. The shear pattern examines the distance from the low level centre to the CDO, with the principle being that greater involvement of the low level centre with the deep convection indicates a stronger system. The CDO appearance is judged on its size and degree of banding.

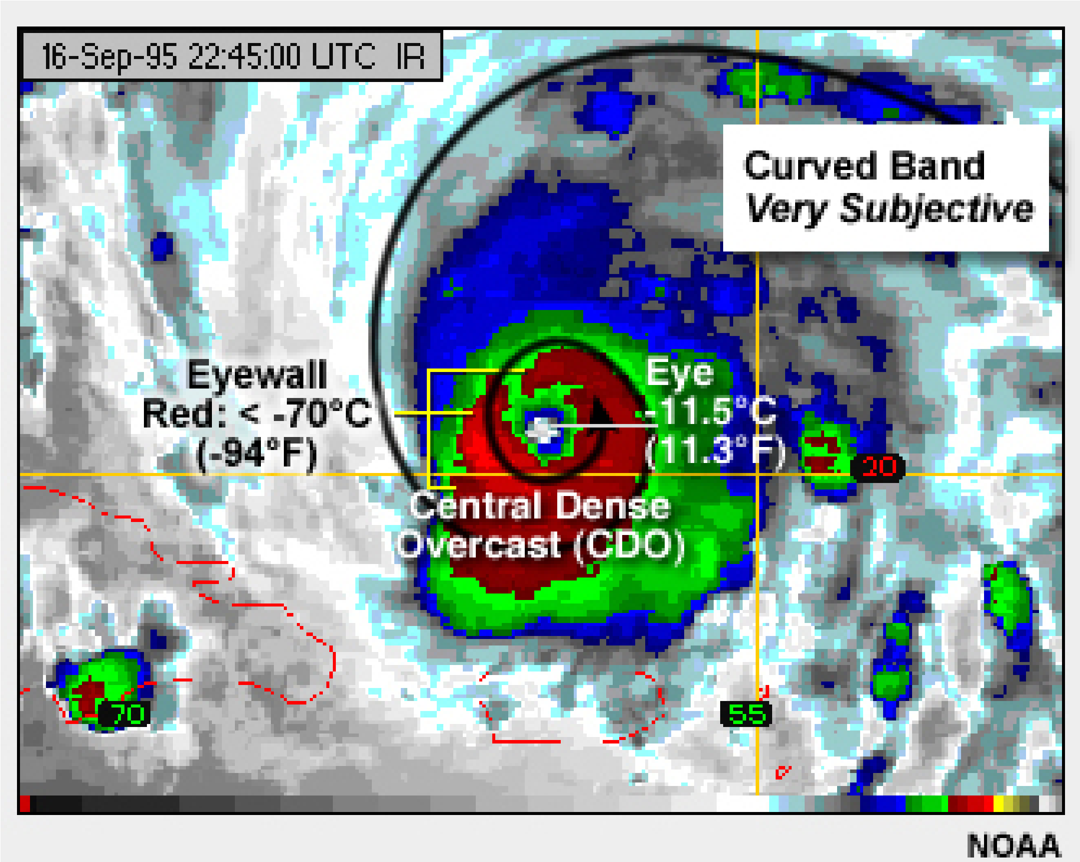

Figure 2Sample identification of the Dvorak eyewall pattern, curved band pattern, and CDO.

CI	**MSW (kts)**	**MSLP (hPa)**	
		Atlantic	West Pacific
1.0	25		
1.5	25		
2.0	30	1009	1000
2.5	35	1005	997
3.0	45	1000	991
3.5	55	994	984
4.0	65	987	976
4.5	77	979	966
5.0	90	970	954
5.5	102	960	941
6.0	115	948	927
6.5	127	935	914
7.0	140	921	898
7.5	155	906	879
8.0	170	890	858

Table 1 Summary of the Dvorak Atlantic and western North Pacific wind-pressure relationships.

The Dvorak Technique has been updated and automated through the use of digital IR data and objective algorithms that are based on the original empirical relationships.

First was the Objective Dvorak Technique (ODT), then the Advanced Objective Dvorak Technique (AODT), and, as of 2006, the Advanced Dvorak Technique (ADT). An example of comparison between aircraft reconnaissance observations of the intensity of Hurricane Ivan (2004) with both the ODT and ADT is presented in Figure 3.

IR analysis is also used to identify annular hurricanes objectively. Annular hurricanes have strong and steady intensities and are generally 10-40% larger than normal hurricanes in the Atlantic and East Pacific. On IR images, annular hurricanes are distinctly symmetric and have a large circular eye surrounded by a nearly uniform ring of deep convection and little deep convection outside of that ring.

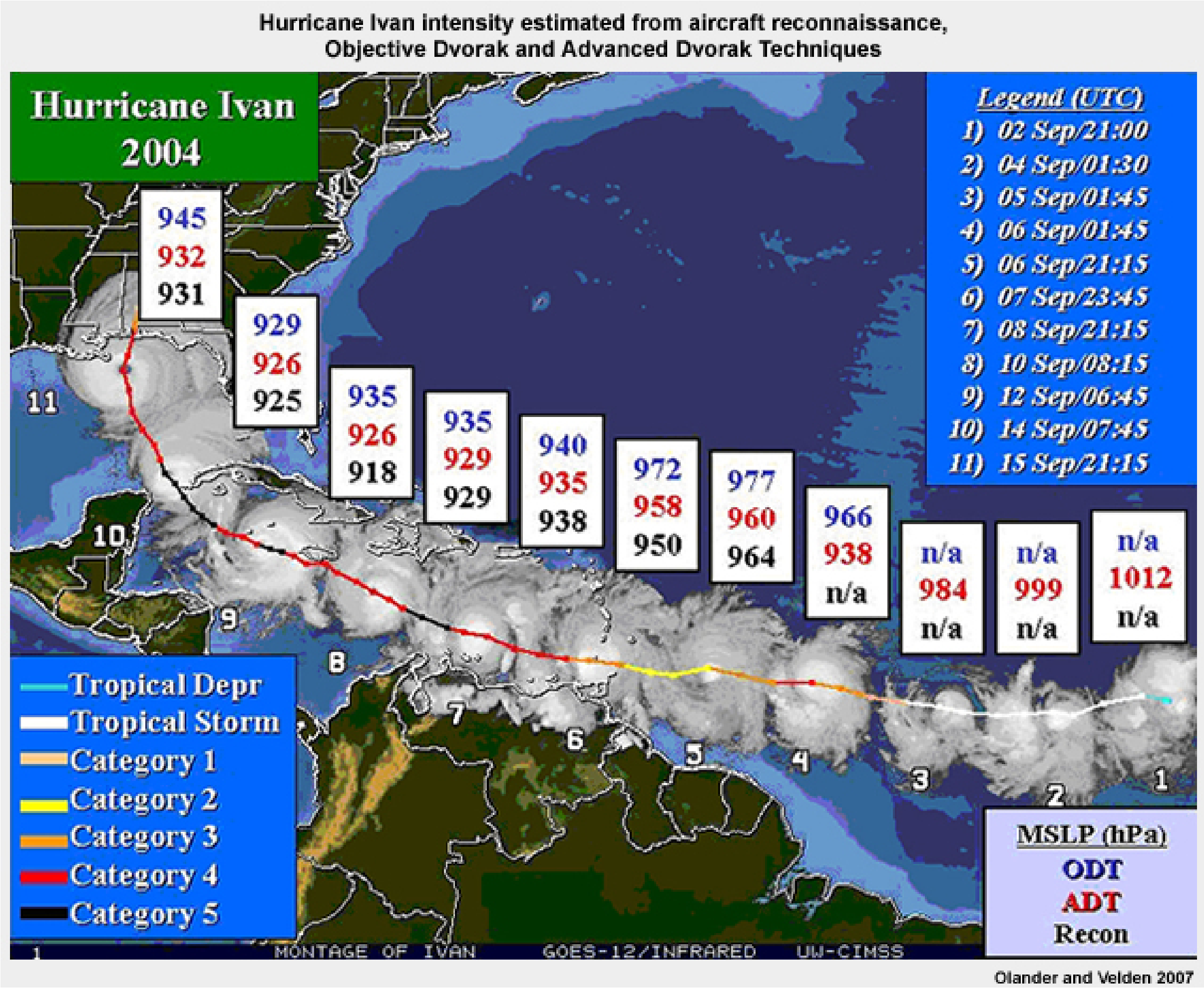

Figure 3 *Hurricane Ivan intensity estimated by aircraft reconnaissance, ODT, and ADT.*

Satellite Microwave Observations

Microwave radiometers can detect the internal cyclone structure, such as the location of the eye, because microwave wavelengths are strongly attenuated by hydrometeors (droplets or ice crystals) inside of the eyewall and rainbands. IR techniques, meanwhile, observe only the cloud tops and thick cirrus can hide the underlying TC structure.

For example, in Fig. 4 (below), it is difficult to identify the eye of Tropical Cyclone Indlala from the IR images (upper panels). However, in the 85 GHz microwave images, the eye is prominent (lower panels), providing a reliable indication of a strengthening tropical cyclone. Moreover, the region of cold cloud to the right of the eye, in the IR image, is not associated with deep convection; it shows up as blue in the microwave image.

Unfortunately, microwave instruments fly on low-earth-orbiting (LEO) satellites which observe the same cyclone at most twice per day. Multiple daily views of the same tropical cyclone have become more common as the network of LEO satellites continues to expand. Because they show the internal structure of TCs, microwave images are helping to identify intense cyclones many of which display concentric eyewall structures.

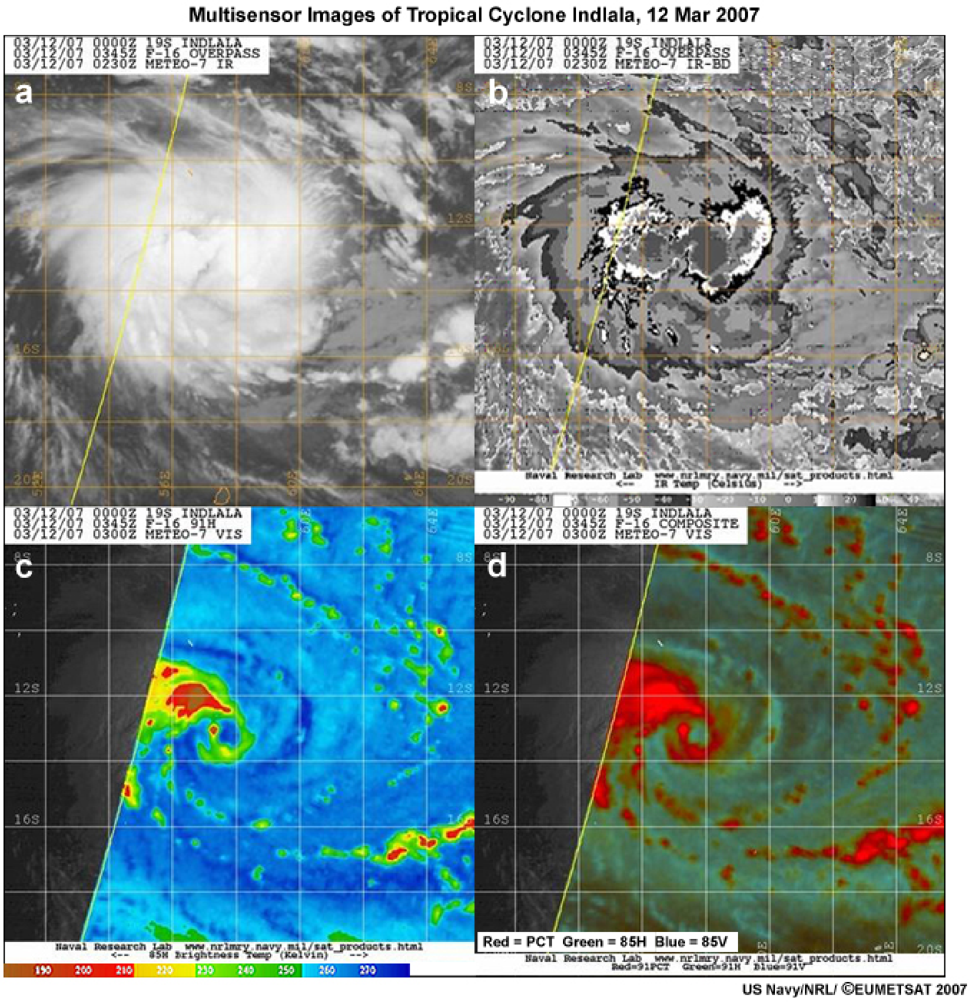

Figure 4Tropical Cyclone Indlala (2007) observed by geostationary grayscale IR and enhanced IR-BD (upper left, right) and polar-orbiting microwave 85 GHz sensor (lower).

Morphed Integrated Microwave Imagery at CIMSS (MIMIC) tries to fill the microwave temporal gap.

MIMIC creates a sequence of synthetic TC microwave images for the periods between actual satellite microwave observations. The technique is based on the general expectation that tropical cyclones are roughly axially symmetric in terms of wind speed. The motion of features is the result of interpolation of images, advection, and rotation as the interpolated images are blended. The morphed images are produced every 15 minutes to match the geostationary-IR routine and are available in real-time for five ocean basins. A sample image, for Hurricane Ivan (2004), is shown in Fig. 5.

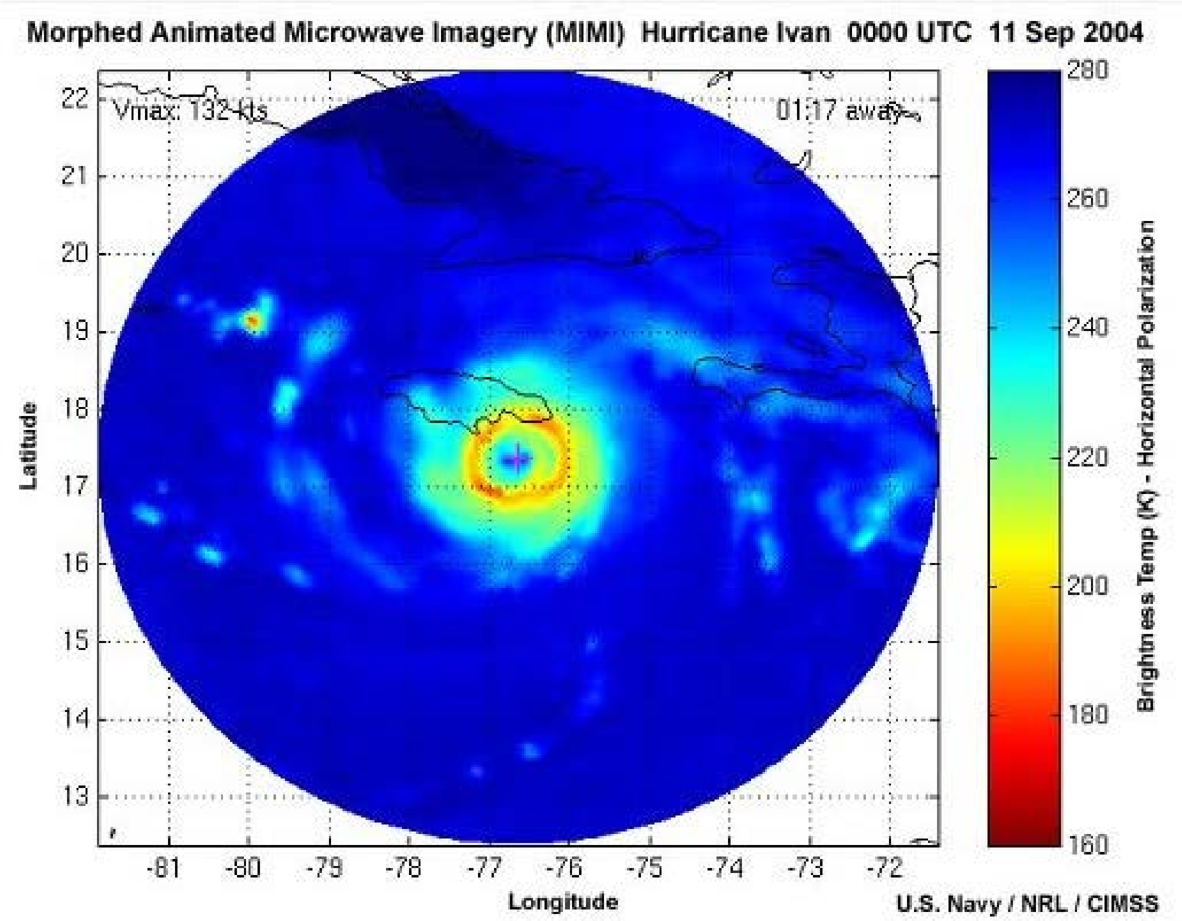

Figure 5MIMIC sequence of morphed and observed microwave images of Hurricane Ivan, September 2004.

MetLink
Royal Meteorological Society

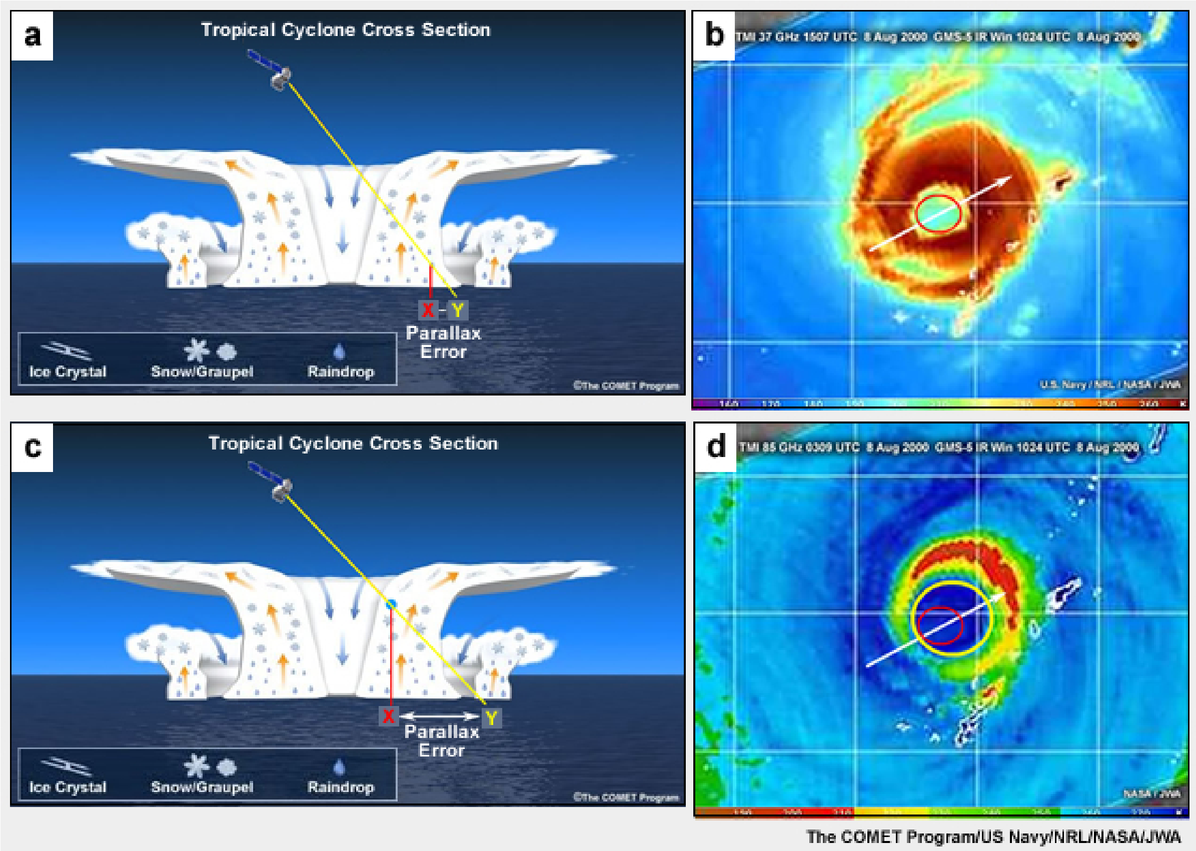

Figure 6Conceptual model of the relative parallax errors in satellite microwave images of (upper) 37 GHz liquid droplet emissions and location of the eye of Typhoon Jelawat (2000) and (lower) same as upper except for 85 GHz ice scattering. The red circle is the

While microwave instruments provide superior TC feature identification, one caveat must be considered in locating the eye of a TC; the effect of parallax. Parallax errors occur when a satellite's slanted viewing angle places features away from their actual location. Figure 6 illustrates how parallax errors differ at 85GHz, which is sensitive to ice scattering at high altitudes, and 37 GHz, which is sensitive to emissions from liquid drops at low altitudes. The parallax error is about 5 km at 37 GHz compared with 10-20 km for 85 GHz. The latter frequency has higher resolution (compare Fig 6, b and d) and is the preferred channel for observing tropical cyclone structure and intensity changes.

Eyewall Replacement Cycles

The concentric eyewall phenomenon or eyewall replacement cycle is often observed during periods of intensification or weakening of intense TCs (those with winds greater than 50 m s^{-1}, 115 mph). In general, TC eyewalls contract as they strengthen to the intense TC threshold. After the existing eyewall has contracted to its minimum size for that threshold intensity, the TC enters a weakening phase. All other factors being equal, the TC weakens when an outer eyewall forms; some of the moisture and momentum is taken from the existing eyewall, which dissipates. The outer eyewall contracts gradually and the TC regains its original strength or becomes stronger.

For example, major Hurricane Ivan weakened, from a category 5 to a category 4, as it approached Jamaica from the southeast, in part because of an eyewall replacement cycle. Two concentric eyewalls are evident in the radar image from Kingston, Jamaica (Fig. 7).

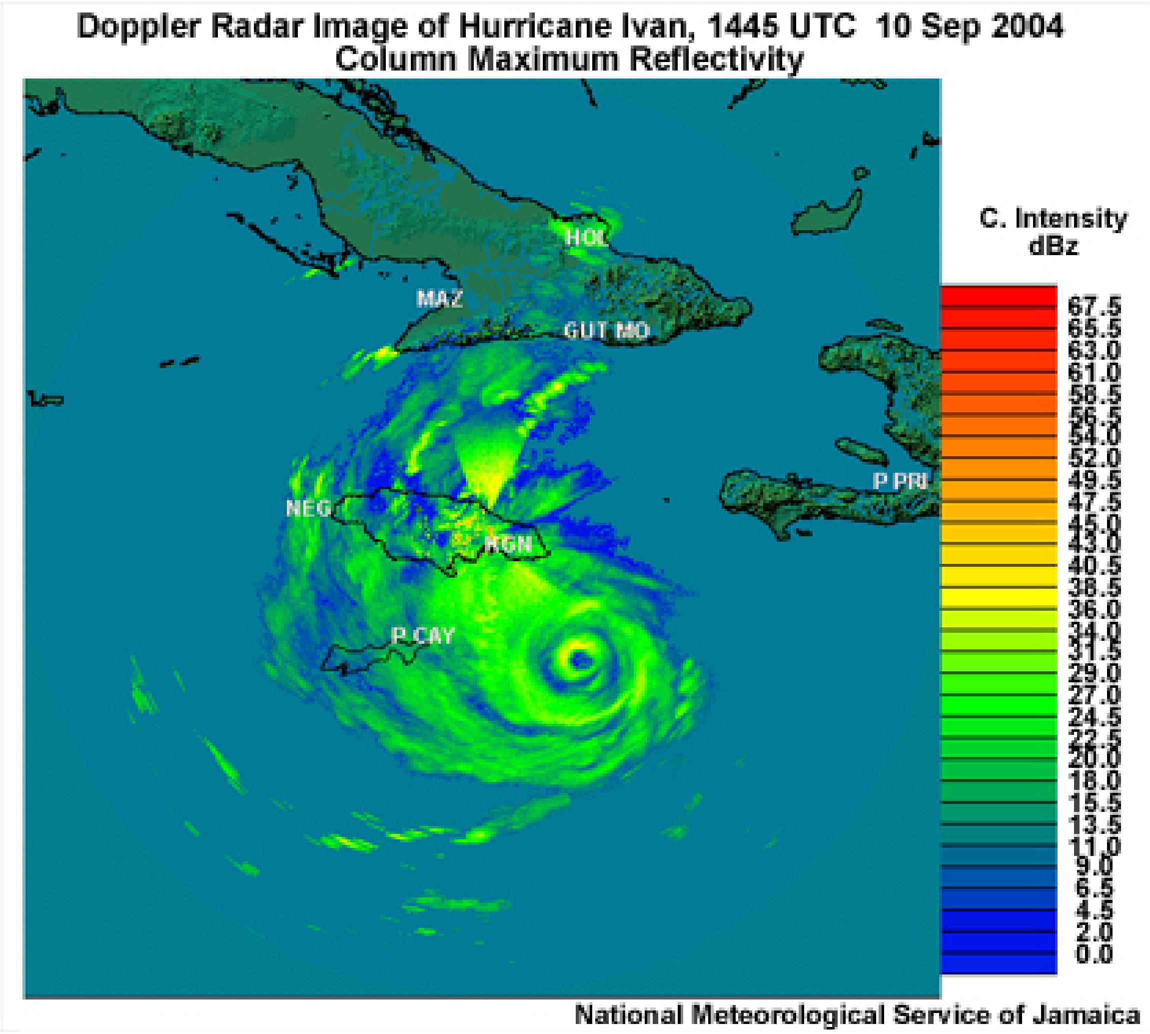

Figure 7 Radar reflectivity image from Kingston, Jamaica at 1445 UTC 10 Sep 2004. Note the two concentric eyewalls that were likely the cause of short term weakening in Ivan. At this time, Ivan had weakened from category 5 to category 4 with sustained winds of 65 m s-1 (125 knots; image courtesy of the National Meteorological Service of Jamaica).

Eyewall replacement cycles can last as short as 12-18 hours to as long as 2-3 days (e.g. Fig. 8). Some intense TCs undergo multiple eyewall replacement cycles. The West Pacific has the largest percentage of intense storms which exhibit double eyewall structure because many can travel longer distances before encountering land, cool SSTs, or other unfavourable environmental conditions.

New satellite analyses are being developed to objectively identify eyewall replacement cycles, using software to extract information from IR images about the onset of eyewall replacement cycles. The IR information, when combined with microwave image data, is being used to create an objective index to calculate the probability of secondary eyewall formation.

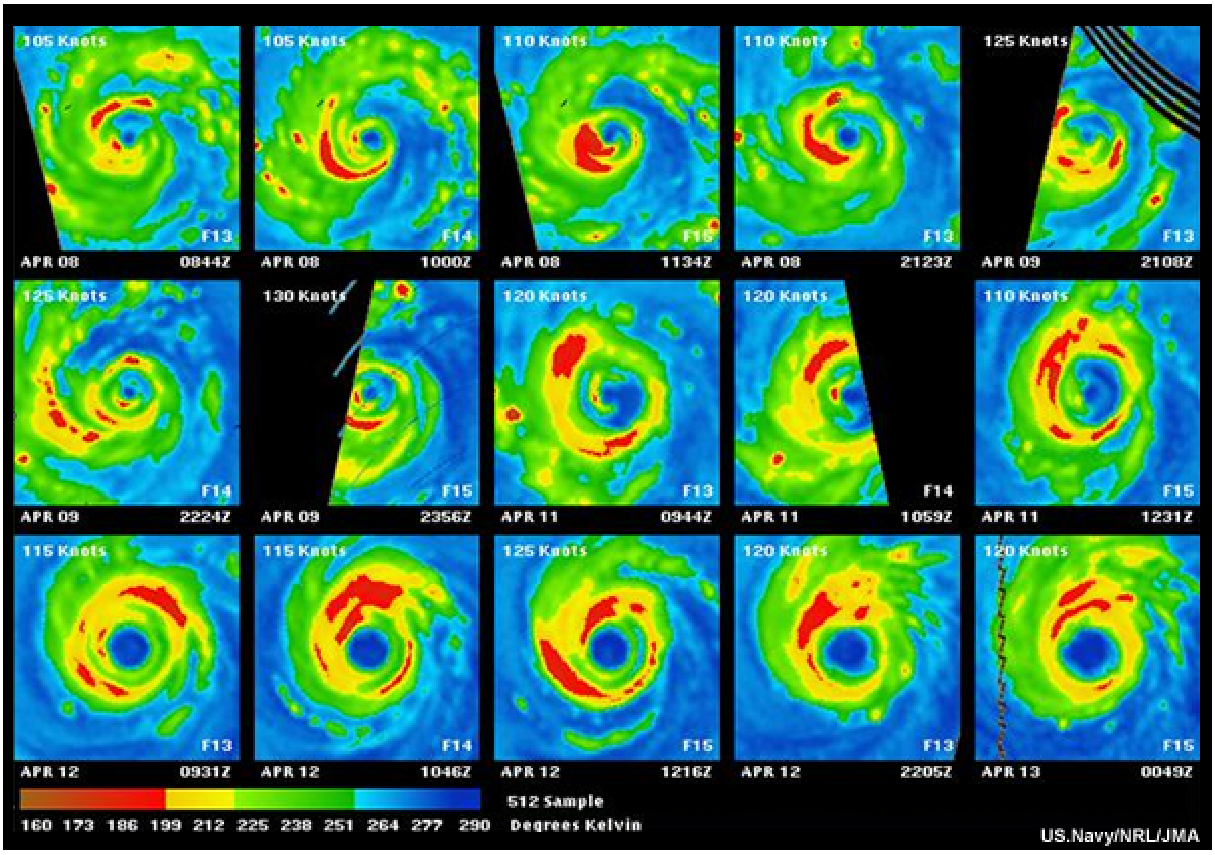

Figure 8Eyewall replacement cycle in Typhoon Sudal in the West Pacific, seen in SSM/I 85 GHz H-Polarized image from 8-13 April 2004.

Satellite-derived Winds

It is important to consider TC intensity not only in terms of the central pressure or the radius of maximum winds but in terms of other wind speed radii that are critical to decision makers. The width of evacuation zones is based on thresholds such as the radius of gale force winds (1-minute sustained surface winds between 17 and 24 m s^{-1}). Wind velocity estimates are also critical to forecasting of storm surge. TC sizes range from Cyclone Tracy (1974), whose radius of gale force winds was only 48 km, to Super Typhoon Tip, which had a gale force wind radius of 1110 km.

Prior to landfall, near surface wind speed and direction are observed by satellite-based microwave scatterometers, which measure the backscatter from small-scale waves on the ocean surface and relate the backscatter to wind velocity. Microwave scatterometers generally perform best in moderate-wind and low-precipitation environments, outside of the high-wind and high precipitation region of the eyewall. Cloud drift winds, although limited by inaccuracies in height assignments, also provide estimates of winds outside of intense convection. Figure. 9 provides examples of satellite-derived winds in and around TCs.

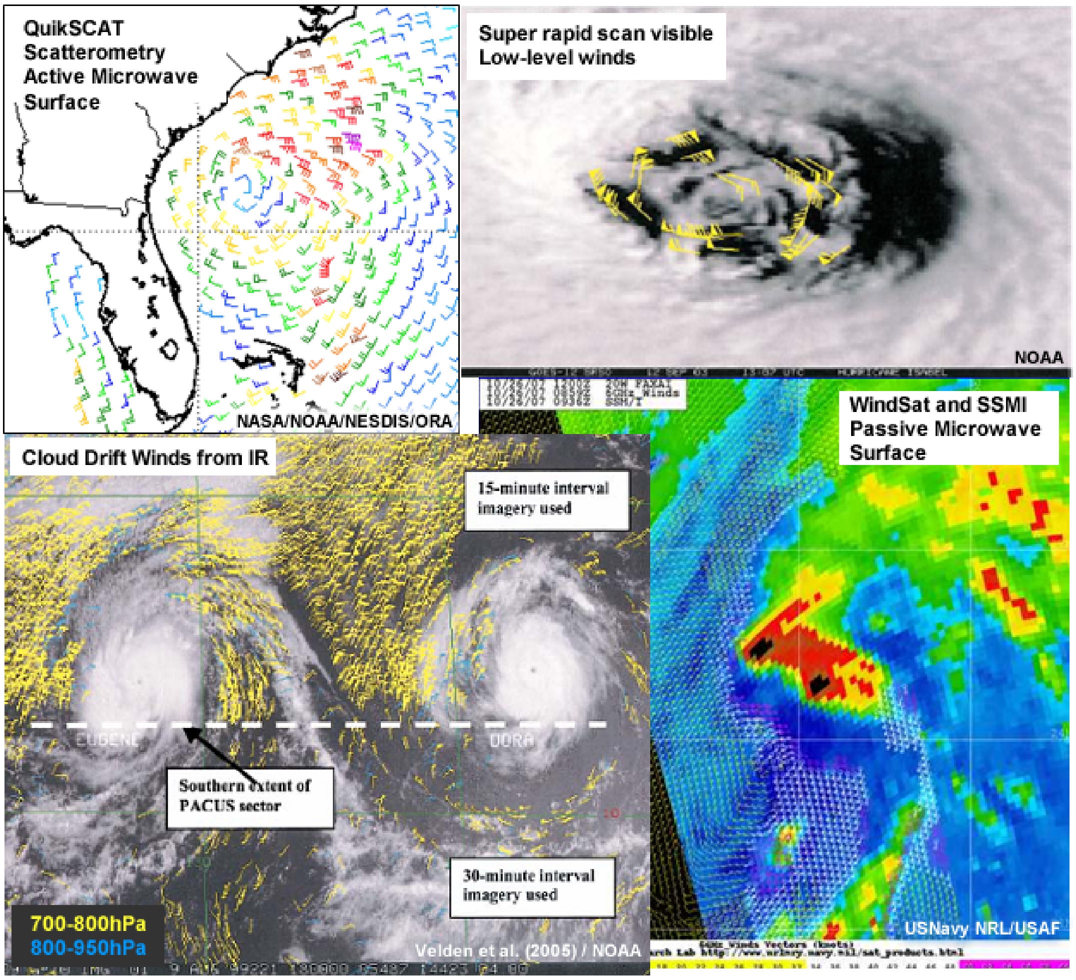

Figure 9 Satellite wind estimates from scatterometer, cloud drift IR images, rapid scan visible images, and passive microwave sensors.

TC Intensity and 34-kt Wind Speed Radius

Statistical relationships between TC intensity estimates from aircraft reconnaissance and satellite IR imagery indicate that the radius of the 34-knot winds could be used to estimate TC intensity. A strong relationship has been found between core intensity and the radius of 34 knot winds. Note that relationship between the 34 knot (17 m s^{-1}) wind radii and intensity is not applicable in all situations as the radius of 34 knot winds is also affected by latitude and number of hours since the TC reached tropical storm intensity. As TCs move to higher latitudes, they tend to become larger.

Remote Sensing of Inner Core Dynamical Features

While eyewalls are often observed to be nearly circular, they are occasionally observed to adopt polygonal shapes. Based on theoretical dynamics, numerical simulations, and liquid water experiments the polygonal structures were hypothesized to be associated with mesovortices. Recent observational studies show pentagon-shaped reflectivity patterns (Fig. 10a, c) associated with mesovortices within the eye (Fig. 10c), confirming their existence. These eyewall mesovortices are deep vortex structures in the eyewall convection and so have much smaller horizontal scale than the eye. Wind speed in eyewall vortices can be 10% greater than the rest of the eyewall. Addition of the flows associated with the mesovortices to the flow in the eye results in the polygonal shape observed in the cloud pattern.

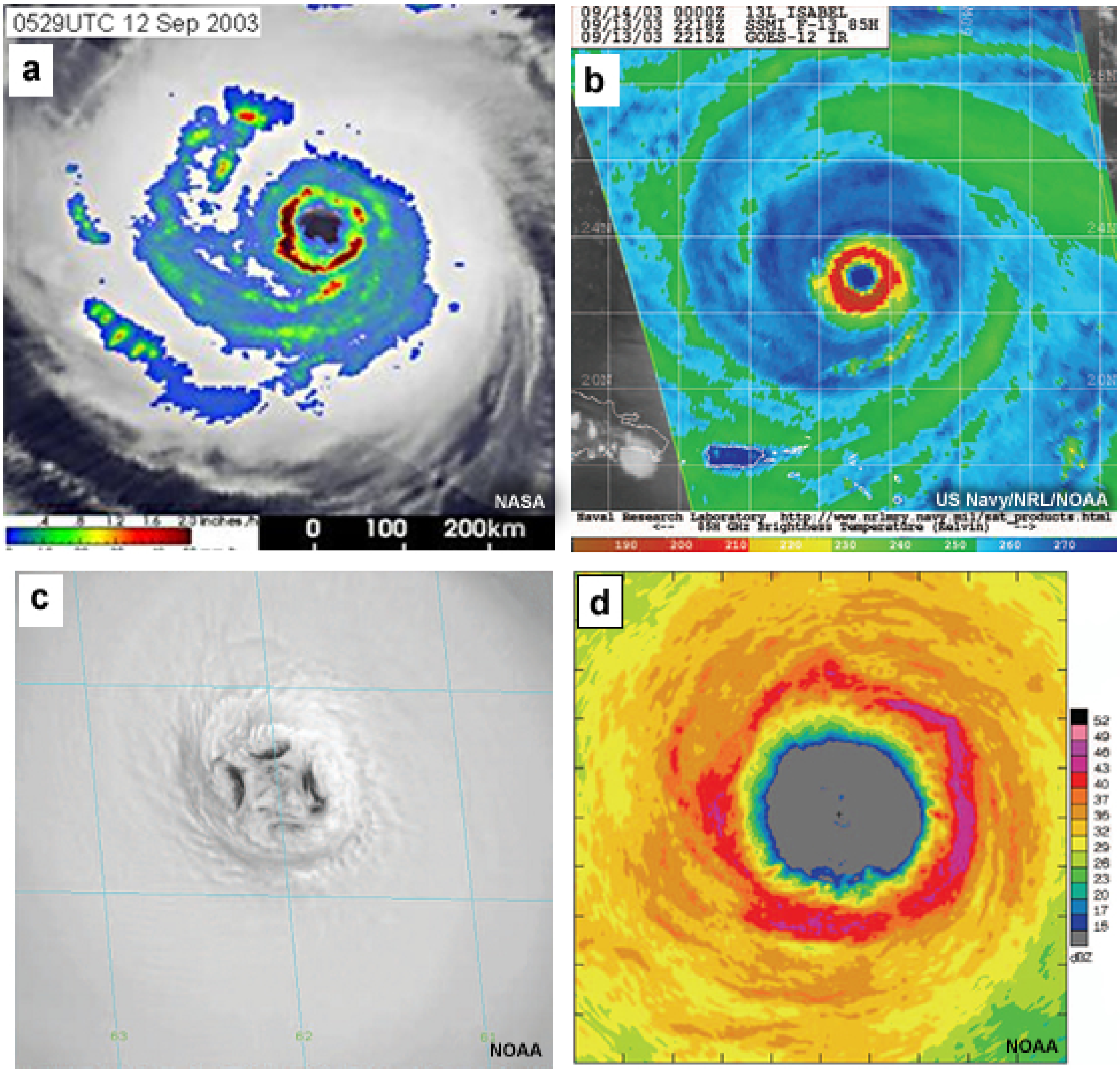

Figure 10 Satellite and airborne radar imagery of Hurricane Isabel. (a) TRMM PR image at 0529 UTC on 12 September 2003; (b) SSM/I 85 GHz brightness temperature at 2218 UTC; (b) visible image at 1745 UTC from GOES super rapidscan operations; and (c) radar reflecti

The 2005 Hurricane Rain band and Intensity Change Experiment (RAINEX) made targeted observations in the inner core of Hurricanes Katrina, Rita, and Ophelia in order to understand how changes in their inner core influenced and were influenced by intensity changes. Fig. 11 shows a number of interesting features hitherto unobserved, such as filaments of very high reflectivity that are oblique to the concentric eyewall and rainbands. These structures are affected by varying winds as they move around the eyewall and provide clues about how eyewalls transform during rapid changes in intensity. They appear to be similar to structures predicted in theoretical studies and numerical models.

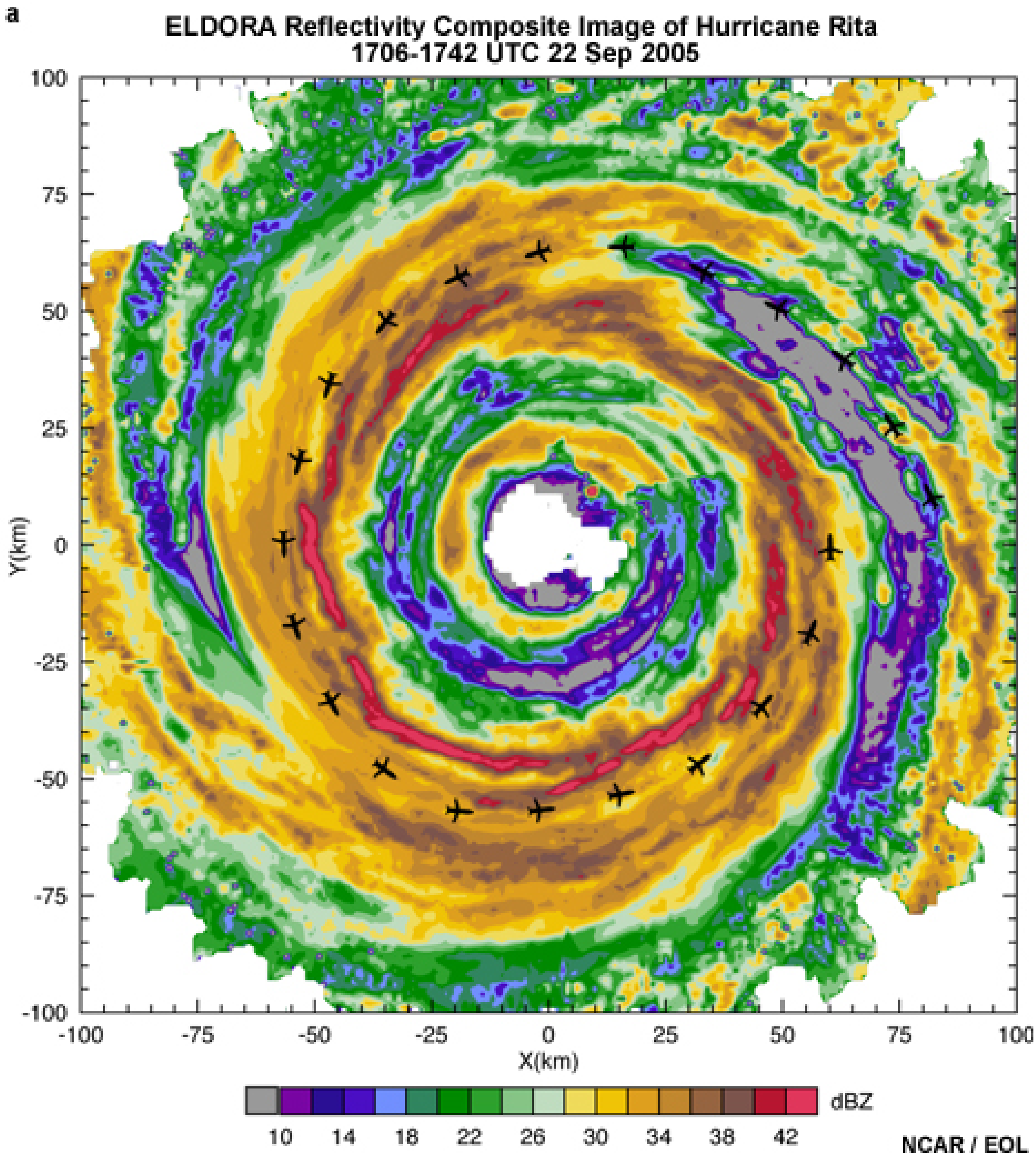

Figure 11 Radar reflectivity composite image of Hurricane Rita taken by ELDORA, 22 Sep 2005, during the Hurricane Rainband and Intensity Change Experiment (RAINEX). The flight track is marked by airplane icons.

How do these mesovortices affect TC intensity? Theoretical models and evidence in the new observations suggest that the mesovortices contribute cyclonic vorticity which is mixed into the eye. This increase in the local vorticity spins up the eye. In addition, the low-level mesovortices create a secondary circulation that transfers air from the eye to the eyewall and provides additional power to the hurricane heat engine.